AIChE

Ultrasonic Processing of Suspensions of Hematite Nanopowder Stabilized with Sodium Polyacrylate

P. Ding and A. W. Pacek
School of Chemical Engineering, University of Birmingham, Birmingham, B15 2TT, U.K.

DOI 10.1002/aic.11899
Published online July 24, 2009 in Wiley InterScience (www.interscience.wiley.com).

The effect of power input, solid content, surfactant concentration, and pH on the kinetics of wet deagglomeration of hematite nanopowder in ultrasonic comminution device and on the rheology of resulting suspensions has been investigated and compared with the kinetics of deagglomeration and rheology of the suspensions of goethite nanopowder. It has been found that the main mechanisms are fragmentation and erosion, which leads to bimodal transient size distributions of aggregates. Fragmentation of large aggregates starts after certain delay time but erosion of nanoparticles starts from very beginning of processing. Deaggregation of hematite nanopowder is only possible in the presence of surfactant, but increase of concentration of surfactant above certain critical value does not affect kinetics of deagglomeration. The increase of solid concentration up to 20 w/w% *reduces the amount of energy necessary for deagglomeration of unit mass of the powder. Effect of pH on the kinetics of deagglomeration and the morphology/rheology of the resulting suspensions is discussed.* © 2009 American Institute of Chemical Engineers *AIChE J,* 55: 2796–2806, 2009
Keywords: hematite nanopowder, ultrasonic energy, surfactant, rheology, pH

Introduction

Hematite is the mineral form of iron oxide (Fe_2O_3). It occurs in different colors (black to silver-gray, brown to reddish brown, or red) and it is commonly used as a pigment. Dispersing dry pigment nanopowders in aqueous solutions is a critical and expensive step in paint manufacturing and the properties of suspensions determine the subsequent operations of the paint formulation, the paint shell life and the quality of painted surfaces.[1,2]

Different types of mixers are used in industry to disperse nanopowder in liquids. The most common are: high-shear mixers, valve homogenizers, colloidal mills, and ultrasound dispersing devices with the later being one of the most efficient.[3] Nanoparticles suspensions can be intrinsically stable (silica nanoparticles[4,5]) or can be easily stabilized by adjusting pH of suspension (goethite nanoparticles[6]). Many types of the nanosuspensions have to be stabilized by addition of different stabilizers[1] and polymers derived from acrylic acid are used for stabilizing the aqueous suspensions of different pigments.[7] The efficiency of stabilization can be related to adsorption isotherms. The adsorption isotherms of polyacrylic acid on aluminum oxide,[8] titanium oxide[9,10] and kaolin nanoparticles[11] as well as the effect of polymer molecular weight on the thickness and stability of adsorbed layer[10,12] have been extensively investigated. However, there is practically no information in an open literature on the effect of polyacrylic acid and pH on deagglomeration kinetics of pigment nanopowders and on the rheology of the resulting suspensions.

In this work, effects of the concentration of hematite nanopowder and sodium polyacrylate, pH and energy input on kinetics of deagglomeration and structure/rheology of the resulting suspensions were investigated and the results are discussed later.

The contents of this article reflect only the author's view.
Correspondence concerning this article should be addressed to P. Ding at p.ding@bham.ac.uk

Experimental

Materials and methods

Dry hematite nanopowder of the specific gravity of 3900 kg m^{-3} was purchased from BASF and it was used without further treatments. Sodium polyacrylate (Na-PAA, supplied by Sigma) of average molecular weight of 5100 kg $kmol^{-1}$ was used to stabilize suspensions and hydrogen chloride and sodium hydroxide were used to adjust the pH. The concentration of dispersant in the suspension was defined in terms of mass of solid, for example 5 *w/w*% of solid and 20 *w/*w_{solid}% of dispersant means 1000 g water, 50 g hematite, and 10 g Na-PAA.

Zeta potential of suspensions was measured using *Zeta-Master* (Malvern Instruments, UK). Nanoparticles/aggregates size distributions were measured using *MasterSizer 2000* (Malvern Instruments, UK) taking refractive index of the hematite of 2.94.[13] Each distribution was an average of three consecutive measurements taken automatically at 30 s intervals. Rheological properties of suspensions were measured using a controlled stress rheometer (TA 1000, TA Instruments, UK) while morphology was analyzed with Environmental Scanning Electron Microscope and an optical microscope.

In dry nanopowder elongated hematite nanoparticles (lengths of the order of 100 nm, Figure 1b) tend to aggregate and form large agglomerates (Figure 1a) ranging from tens to hundreds of microns. In majority of applications those large agglomerates have to be broken into single nanoparticles or nanoaggregates.

Experimental rig and procedure

The experimental rig, described in details elsewhere[6] consisted of an ultrasonic processor (Dr. Hielscher GmbH, Germany) connected in a loop with a jacketed stirred vessel via a peristaltic pump. The total volume of the suspension in the rig was 350 ml (V_t) and the volume of the ultrasonic cell (V_{cell}) was 80 ml. The suspension was circulated in the rig at a constant flow rate of 10 ml s^{-1} and the sampling port was placed in the pipe just after the outlet from the ultrasonic cell. Ultrasonic power input was estimated by operating the ultrasonic processor as a crude calorimeter and by measuring the increase of water temperature at different amplitude and cycles over a fixed time interval.[14]

In this work, the kinetics of deagglomeration was analyzed in terms of energy dissipation rate and energy density related to the volume of suspension (E_v) or to the mass of solid (E_w):

$$E_v = \frac{P \cdot t_r}{V_{cell}} \quad \text{or} \quad E_w = \frac{P \cdot t_r}{W_S} \tag{1}$$

where P is power input, W_S mass of solid in the flow cell and t_r is the mean residence time in the cell calculated from:

$$t_r = \frac{t_t}{(1 + \frac{V_t - V_{cell}}{V_{cell}})} = t_t \cdot \frac{V_{cell}}{V_t} \approx 0.23 \cdot t_t \tag{2}$$

Kinetics of deagglomeration can also be analyzed in terms of energy density in the ultrasonic cell and number of passes of the suspension through the cell. Both approaches are equivalent and the number of passes can be easily related to the flow rate and volume of the system.

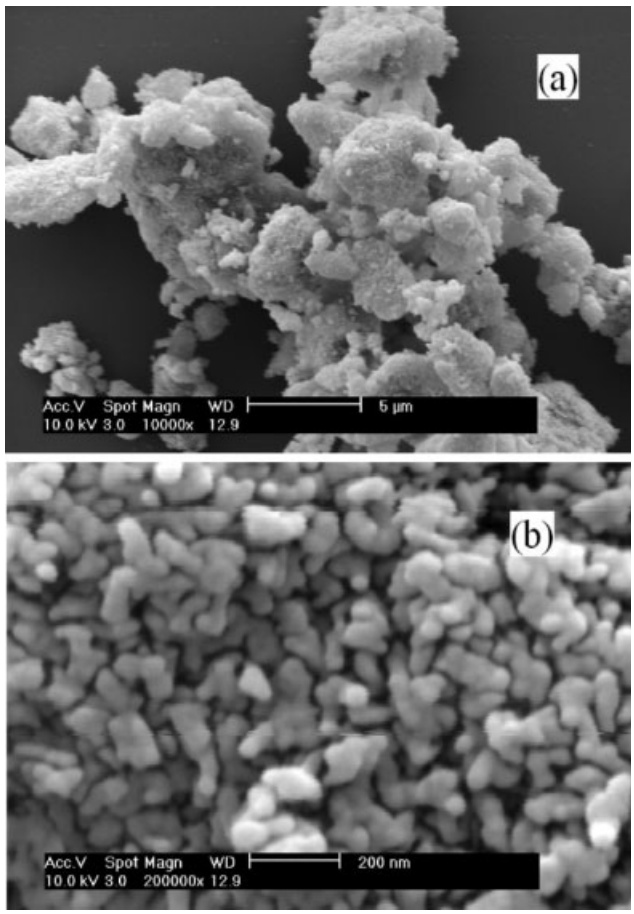

Figure 1. Morphology of hematite nanopowder: (a) Large aggregates of dry powder and (b) nanoparticles on the surface of those aggregates.

Two sets of experiments were carried out. In the first set, the effects of:

- dispersant concentration (1, 5, 10, and 20 *w/*w_{solid}%) at solid concentration of 5 *w/w*% and pH = 9,
- solid concentration (5, 10, 20, and 30 *w/w*%) in 20 *w/*w_{solid}% Na-PAA solution at pH = 9,
- total power input (39 W, 50 W, and 66 W) to the suspension of 5 *w/w*% hematite in 20 *w/*w_{solid}% Na-PAA solution at pH = 9, on the kinetics of deagglomeration were investigated. The suspension of hematite nanopowder in dispersant solution was premixed in the stirred vessel at impeller speed between 650 and 1050 rpm depending on the concentrations of nanopowder. pH was adjusted to a required value and the suspension was circulated through a flow cell fitted with sonotrode. Small samples of the suspensions were withdrawn at certain time intervals and aggregates/nanoparticles size distributions were measured and morphology of suspensions was analyzed.

In the second set of experiments, the reversibility of pH effect on rheology and morphology of suspensions of hematite nanoparticles was investigated. 5 *w/w*% solid has been

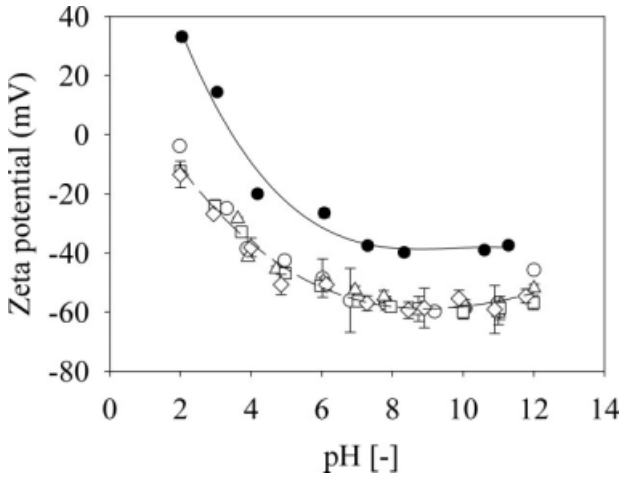

Figure 2. Zeta potential of hematite nanoparticles as a function of pH at different dispersant (Na-PAA) concentrations: (●) 0.0 w/w_{solid}%, (○) 1 w/w_{solid}%, (Δ) 5.0 w/w_{solid}%, (□) 10.0 w/w_{solid}%, and (◇) 20.0 w/w_{solid}%.

suspended in a 20 w/w_{solid}% Na-PAA solution at pH = 9 and has been processed for 2 h at a power input of 66 W. After that time, all aggregates were broken and only single nanoparticles/small aggregates were suspended in the liquid. Next, pH was increased stepwise from 9 to 10 and 12 followed by stepwise reduction to 10, 8, 7, 5, and finally to 3. After pH reached 3, it was increased again to 5, 7, and finally to 9. At each pH, the suspension was processed for 20 min at the constant energy dispassion rate and after that time small sample was taken and agglomerate size distributions, morphology, and rheology were analyzed. In all experiments, the temperature of the suspension was kept constant at 20°C.

In both sets of experiment, the maximum total processing time was 2 h and under most experimental conditions 100% of nanopowder was dispersed into nanoparticles.

Results and Discussion

Zeta potential

Zeta potential of hematite nanoparticles was measured at different pH and at different Na-PAA concentrations. The results are summarized in Figure 2.

Isoelectric point (IEP) of nanoparticles in dispersant free suspension was close to 3.5, much lower than 8–9 reported by Holmberg[15] and 5.5 reported by Nsib et al.[1] Discrepancies between literature data and our results are probably due to differences in materials grade, batch number and possibly manufacturing procedures. It has been reported that very small amount of acid added during the production of iron oxide can reduce IEP dramatically.[16]

The addition of 1 w/w_{solid}% of Na-PAA increases absolute value of the zeta potential of hematite nanoparticles by ~20 mV but, further increase of concentration of Na-PAA to 20 w/w_{solid}%, did not affect zeta potential. The initial increases of absolute value of zeta potential are caused by adsorption of the anionic polymer on the surface of the particles. However, at polymer concentration sufficient for full coverage of nanoparticles surface, zeta potential is independent of the concentration or molecular weight of the polymer.[1,10]

Transient size distributions

Figure 3a shows transient size distributions measured during deagglomeration of 5 *w/w*% hematite nanopowder suspended in 20 w/w_{solid}% Na-PAA solution at pH = 9. Each curve in Figure 3a was obtained as an average of three consecutive measurements of size distributions taken automatically by MasterSizer at 30 s intervals. The inset showing all three measured distributions clearly indicate that in the presence of surfactant, the suspension was stable. Similar transients were observed in all experiments at pH between 7 and 12 in the presence of dispersant. Dry nanopowder was completely agglomerated with the agglomerates ranging from 300 nm to ~100 μm and single modal size distribution with

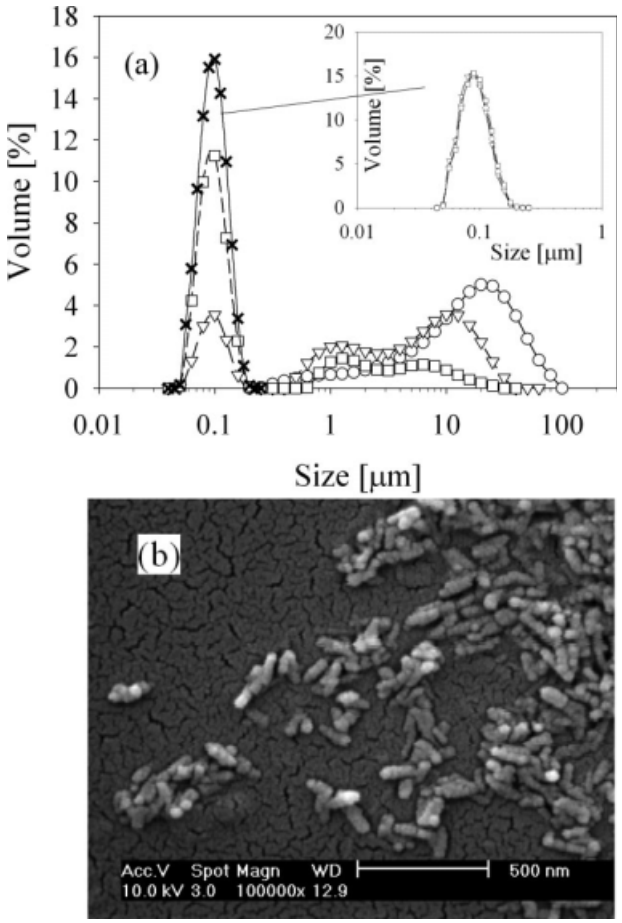

Figure 3. (a) Transient size distributions during deagglomeration of 5 *w/w*% hematite nanopowder suspended in 20 w/w_{solid}% Na-PAA solution at pH = 9: (a) (○) 0 min (0 MJ m^{-3}), (▽) 10 min (113 MJ m^{-3}), (□) 60 min (678 MJ m^{-3}), (×) 120 min (1356 MJ m^{-3}), and inset: size distributions in the sample taken after 120 min during measurements in MasterSizer and (b) morphology of hematite nanopowder after deagglomeration was completed.

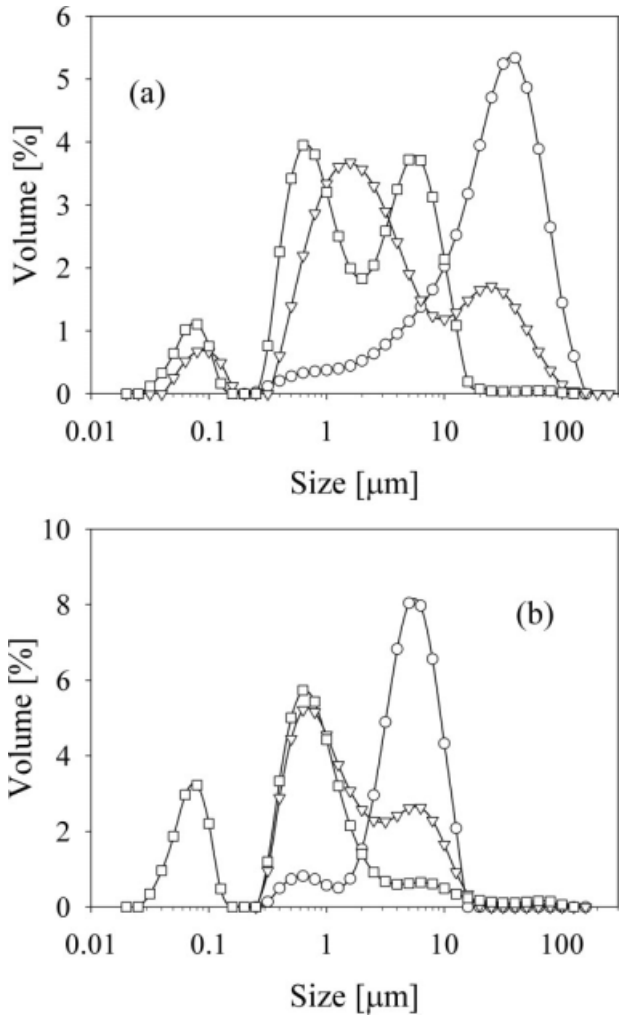

Figure 4. Size distribution at pH = 9, 5 *w/w*% solid, 0 *w/w*% Na-PAA, and 824 kW m^{-3}: (a) Size distribution at different processing time, (○) 0 min, (▽) 30 min, and (□) 120 min and (b) size distributions in the sample taken after 120 min during measurement in MasterSizer, *t* = 0 (○), (▽) *t* = 30 s, and (□) *t* = 60 s.

the median of ~20 μm (see Figure 3a). Those agglomerates were gradually broken by fracture and erosion as indicated by bimodal size distributions with the second mode corresponding to agglomerates and first mode corresponding to nanoparticles/nanoaggregates.[5,17,18]

Once the nanopowder was completely dispersed size distribution became single modal with median size of 100 nm corresponding either to the length of single nanoparticle (100 nm) or to nanoaggregates consisting of a few nanoparticles (see Figure 3b). The bimodal transient size distributions cannot be analyzed in terms of the mean sizes; therefore, the analysis of both modes was carried out separately. The first mode was analyzed in terms of cumulative volume fraction of fines (here fines means nanoparticles and nanoaggregates smaller than 300 nm) and the second mode of volume distribution was analyzed in terms of the average size (d_{50}) of the aggregates large than 300 nm.

Deagglomeration 5 *w/w*% suspension at the same average energy dissipation rate and pH but without dispersant was also investigated and the results are summarized in Figure 4. Transient size distributions measured in the samples taken at different processing times are shown in Figure 4a. The results of all three measurements of the size distribution in the sample taken after 120 min shown in Figure 4b prove that in the absence of dispersant, the suspension is very unstable (compare inset in Figures 3a and 4b). These results also question the accuracy of the distributions shown in Figure 4a and confirm well known fact that aqueous suspensions of hematite nanopowder have to be stabilized with appropriate surfactant. The efficiency of the stabilization strongly depends on pH (see Figures 8, 9, 11, and 12). Industrial application of the aforementioned findings has been recently discussed by the authors.[14,19]

The effect of energy input on kinetics of deagglomeration

The kinetics of breakage of large agglomerates has been quantified using an empirical energy-size reduction model:

$$d_{50} = C \cdot E_v^{-\alpha} \tag{3}$$

This model has been commonly used to relate mean diameters to the energy input in different comminution processes, for example breakage of dolomite aggregates[20] and Al_2O_3 aggregates in a stirred ball mill,[21] deagglomeration of silica nanopowder in a high-shear mixer,[5] and deagglomeration of goethite nanopowder in an ultrasonic device.[17]

In majority of industrial applications hematite suspensions of nanopowder are stabilized by addition of dispersant and adjustment of pH of the suspension, whereas the suspensions of goethite nanopowder are stabilized by pH adjustment only. In Figure 5, the kinetics of deagglomeration of hematite nanopowder suspended in 20 w/w_{solid}% Na-PAA solution at pH 9 is compared with kinetics of deagglomeration of goethite nanopowder suspended in water at pH = 3.

The median diameters (d_{50}) of hematite aggregates corresponding to the second mode of volume distributions (see Figure 3a) as a function of energy density at different energy dissipation rates are shown in Figure 5a and compared with transient median diameters of goethite (different form of iron oxide) aggregates.[17]

From Figure 5a, it is clear that the fracture of hematite aggregate requires much more energy than the fracture of goethite aggregates. Although the fracture of goethite aggregates starts at very low-energy density (at the very beginning of comminution), the fracture of hematite aggregates starts only after certain amount of energy was put into the suspension, for example after certain delay time. Similar delay time during comminution was reported by Kusters et al.,[22] who postulated that this time is necessary for cracks formation and that the aggregates can only break after sufficiently large cracks are formed. The experimental data indicate that the energy necessary for cracks development is of the order of 10 MJ m^{-3} of goethite and of the order of 150 MJ m^{-3} of hematite. Once this critical amount of energy is put into the suspension, the reduction of aggregates size is well correlated with Eq. 3 as illustrated in Figure 5a. The coefficients in Eq. 3 were calculated by nonlinear regression and for

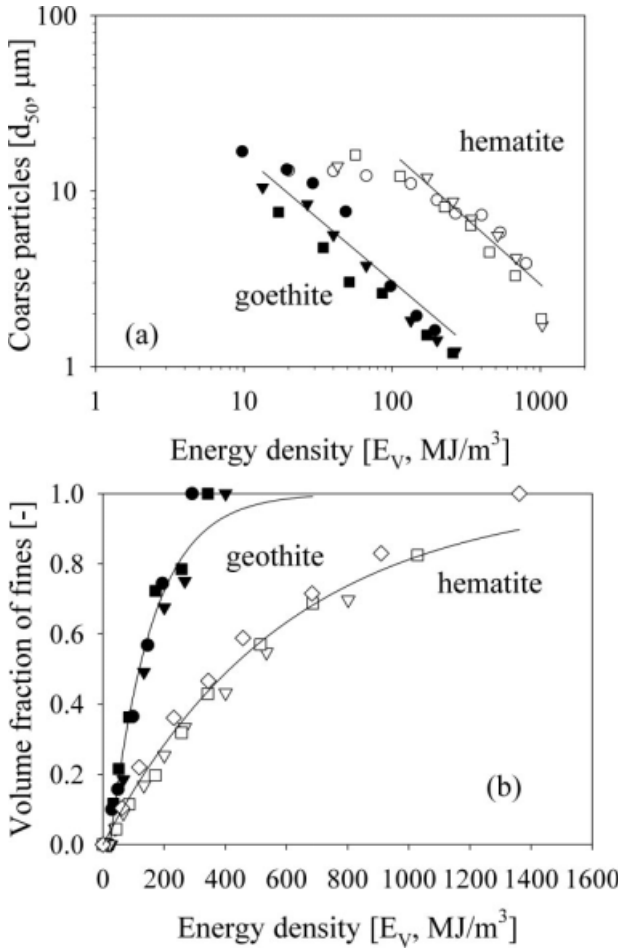

Figure 5. Effect of energy density on: (a) breakage of large aggregates and (b) cumulative volume fraction of fines in 5 *w/w*% solid suspensions at different energy dissipation rate (○) 488 kW m^{-3}, (▽) 625 kW m^{-3}, and (□) 824 kW m^{-3}.

Full symbols—goethite nanopowder, empty symbols-hematite nanopowder.

goethite all experimental points were used whereas for hematite only the points at energy density higher than 100 MJ m^{-3}. For both powders exponent α is ~0.8 and similar values were reported in literature for dolomite suspension in ball mill[20] and for corundum in a stirred media mill.[21] C depends on material/aggregate strength and from experimental results in Figure 5, $C = 528.4$ μm MJ$^{\alpha}$ m$^{-3\alpha}$ for hematite aggregates and $C = 82.2$ μm MJ$^{-\alpha}$ m$^{-3\alpha}$ for goethite aggregates. Considering that C can be interpreted as equilibrium aggregate size at unit energy density this means that hematite aggregates are more than six times stronger than goethite aggregates.

Cumulative volume fraction of fines (f_p) generated by erosion from the surface of agglomerates has been analyzed using model developed by Kusters et al.[18] and recently modified by Ding and Pacek.[17]

$$f_p = 1 - \exp[-\beta \cdot E_v] \quad (4)$$

The cumulative volume fraction of hematite fines generated at different energy dissipation rates are summarized in Figure 5b and compared with cumulative volume fraction of goethite fines at the same energy dissipation rates.[17] From this figure, it is clear that fines generation is much slower in case of hematite nanopowder (erosion constant $\beta = 1.6 \times 10^{-3}$ m^3 MJ^{-1}) than in case of goethite nanopowder, where erosion constant $\beta = 7.0 \times 10^{-3}$ m^3 MJ^{-1} (Ref. 17) that confirms that hematite aggregates are much stronger than goethite aggregates.

The experimental results summarized in Figure 5 show that, on one hand, fracture of large aggregates did not start until the energy input reached ~100 MJ m^{-3} (Figure 5a), for example fracture starts after certain delay time. On the other hand, the erosion of nanoparticles was observed practically from the very beginning of the process as shown in Figure 5b. In this respect, the mechanism of deagglomeration of hematite nanopowder differs from mechanism of deagglomeration of goethite nanopowder where delay time during erosion was not significant.[17]

As discussed earlier, the full description of deagglomeration of hematite nanopowder requires separate analysis of fracture of large agglomerates and erosion of single nanoparticles/nanoaggregates or complete solution of the model based on population balance. However, as in many industrial dispersion processes, the key parameter is the percentage of powder present in the form of single nanoparticles/nanoaggregates further discussion of kinetics of deagglomeration is limited to the analysis of fines generation by erosion.

Effect of Na-PAA concentration on kinetics of fines generation

Effect of dispersant concentration on fines generation in 5 *w/w*% solid suspension at pH = 9 was investigated and the results are shown in Figure 6. The concentration of dispersant is defined in terms of mass of solid, for example mass of dispersant divided by mass of solid (see Experimental section).

Increase of dispersant concentration from 1 to 5 w/w_{solid}% led to the increase of erosion constant β from 0.0011 m^3 MJ^{-1} at 1 *w/w*% to 0.0017 m^3 MJ^{-1} at 5 w/w_{solid}% and consequently to the increase of cumulative volume fraction of fines by 20%. Further increase of Na-PAA concentration from 5 to 20 w/w_{solid}% did not change erosion constant significantly $\beta =$ 0.0018 m^3 MJ^{-1} at 10 *w/w*% and 0.0019 m^3 MJ^{-1} at 20 *w/w*%; therefore, the increases of cumulative volume fraction of fines were also marginal. It appears that at 1 w/w_{solid}% Na-PAA, the surface of nanoparticles is not completely covered.[29–31] It has been reported that viscosity of the suspension is higher when surface of the particles is only partially covered by surfactant than when the surface is covered by continuous layer of surfactant.[1,11,23] The viscosity of the suspension containing 1 w/w_{solid}% Na-PAA (1.47 mPa) was marginally higher than viscosities of suspensions at higher Na-PAA concentrations (1.26 mPa s at 5 w/w_{solid}%, 1.27 mPa s at 10 w/w_{solid}%, and 1.35 mPa s at 20 w/w_{solid}%). Although the differences between viscosities is very small and might be within experimental error, trend of changes supports the hypothesis that at 1 w/w_{solid}% Na-PAA, the surface of the nanoparticles is not completely covered.[29]–31 This leads to the higher interparticle attractive force, and to the lower deagglomeration rate seen in Figure 6. Both viscosity measurements and the fines generation curves indicate that full coverage has been reached

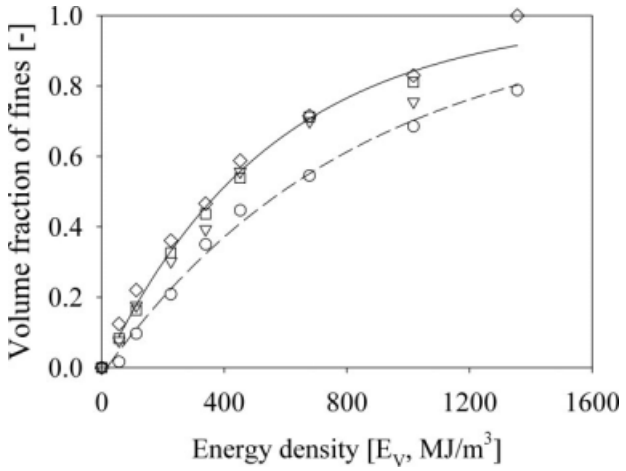

Figure 6. Cumulative volume fraction of fines in 5 *w/w*% suspension at pH = 9 at different Na-PAA concentrations: (○) 1 *w/w*$_{solid}$%, (▽) 5.0 *w/w*$_{solid}$%, (□) 10.0 *w/w*$_{solid}$%, and (◇) 20.0 *w/w*$_{solid}$%.

at 5 *w/w*$_{solid}$% Na-PAA. However in industrial application 20 *w/w*$_{solid}$% Na-PAA is common.

Effect of solid concentration on kinetics of fines generation

The effect of the solid concentration on the kinetics of fines generation has been investigated in suspensions containing 20 *w/w*$_{solid}$% Na-PAA at the power input of 66 W. The cumulative volume fraction of fines are shown both as a function of energy density related to volume of suspension (E_V, Figure 7a) and as a function of energy density related to mass of solid (E_W, Figure 7b).

Figure 7a shows that as the solid load increases the erosion constants decrease ($\beta = 0.002$ m^3 MJ^{-1} at 5 *w/w*%, 0.001 m^3 MJ^{-1} at 10 *w/w*%, 0.0008 m^3 MJ^{-1} at 20 *w/w*% and 0.0006 m^3 MJ^{-1} at 30 *w/w*%) and cumulative volume fraction of fines also decrease. If the energy density is defined in terms of mass of solid (Figure 7b), the increase of solid load leads to the increases of erosion constant ($\beta = 0.098$ kg MJ^{-1} at 5 *w/w*%, $\beta = 0.139$ kg MJ^{-1} at 10 *w/w*%, $\beta = 0.174$ kg MJ^{-1} at 20 *w/w*% and $\beta = 0.189$ kg MJ^{-1} at 30 *w/w*%) and to the increase of cumulative volume fraction of fines. The increase of solid load from 5 to 20 *w/w*% leads to a sharp increase of cumulative volume fractions of fines; however, further increase of solid concentration from 20 to 30 *w/w*% does not significantly affect cumulative volume fraction. These results have important practical applications as they clearly show that rather than processing nanopowders in several batches at low-volume fraction of solid time and energy, it can be saved by increasing the volume fraction of solid and reducing the number of batches. One needs to stress that optimal composition of suspension might depend on the type of the nanopowders. Similar results were reported for goethite nanopowders[17] and were explained in terms of efficiency of utilization of ultrasound energy in concentrated suspensions. During ultrasound dispersion only aggregates that are close to collapsing cavities are broken by the forces resulting from large pressure gradients and/or from high-velocity liquid jets generated by collapsing cavities. Therefore as the concentration of solid increases, the probability of strong interaction between collapsing cavities and aggregates leading to breakage also increases. However, the increase of solid concentrations leads to an increase of the viscosity of suspension (see Figure 10), which increase energy dissipation rather than increasing efficiency of breakage. As the viscosity of suspension increases, the amount of mechanical energy released during collapse of bubbles is reduced and the efficiency of the ultrasonication is also reduced.[2] Therefore, there seems to be an optimal concentration of nanopowder in suspension at which mechanical efficiency of ultrasonication reaches maximum. This concentration depends on the physical properties of nanopowders.

Effect of pH on kinetics of fines generation and morphology of suspensions

pH = 4–12. Figure 8 shows fines volume fraction as a function of energy density at pH = 4, 9, and 12.

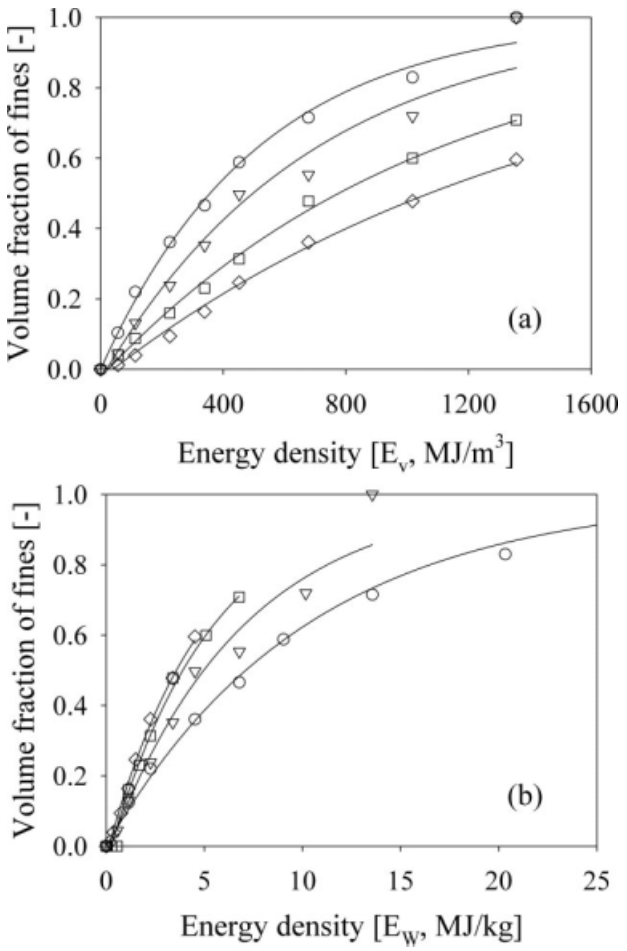

Figure 7. Effect of concentration of hematite nanopowder on the cumulative volume fraction of nanoparticles in 20 *w/w*$_{solid}$% Na-PAA solution at pH = 9; (a) energy per unit volume of suspension and (b) energy per unit mass of solid. (○) 5 *w/w*%, (▽) 10 *w/w*%, (○) 20 *w/w*%, and (◇) 30 *w/w*%.

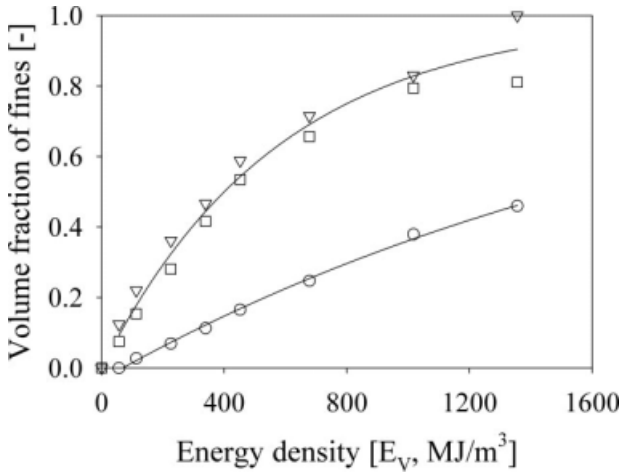

Figure 8. Effect of pH on cumulative volume fraction of nanoparticles in 5 *w/w*% solid suspended in 20 w/w_{solid}% Na-PAA solution, (○) pH = 4, (▽) pH = 9, and (□) pH = 12.

At a given energy density, the cumulative volume fraction of fines drastically increases as pH increases from 4 to 9. Further increase of pH to 12 has practically no effect on fines generation. It appears that fines generation pattern follows the changes of electrostatic repulsive forces or zeta potential. At pH = 4 (zeta potential = −35 mV), the electrostatic repulsive force is small; therefore, the net attractive interparticle force (sum of van der Walls and electrostatic forces) is high which leads to low-erosion rate. The increase of pH from 4 to 9 leads to increase of absolute value of zeta potential from 35 to 60 mV, which indicates the higher electrostatic repulsive force, therefore to the reduction of net attractive force. This makes erosion of single nanoparticles easier and leads to increase of the cumulative volume fraction of fines. Additionally, higher repulsive forces increase stability of nanoparticles by preventing reagglomeration. Further increase of pH to 12 leads to small reduction of zeta potential (electrostatic repulsive force), therefore cumulative volume fraction of fines practically does not change significantly.

pH = 3. At pH = 3, transient size distributions and morphology of suspension (Figure 9) were very different from those observed at higher pH.

Before ultrasonication, the aggregates between 300 nm and 200 μm were observed in the suspension. At low-energy density (226 MJ m^{-3}) part of the largest aggregates (between 10 and 100 μm) was broken and the volume fraction of aggregates below 2 μm increased but single nanoparticles were not observed as indicated by the size distribution in Figure 9a. As the energy density increased to 1356 MJ m^{-3}, the volume of small aggregates (below 2 μm) was reduced (indicating reaggregation) and volume of large agglomerates was also reduced (indicating breakage), for example at this value of pH simultaneous fragmentation/erosion and reaggregation of microaggregates occur.

The morphology of the suspension before ultrasonication (Figure 9b) shows large, relatively compact agglomerates (black flocks on the images). At 226 MJ m^{-3} (Figure 9c), the number and the size of those flocks decreased and

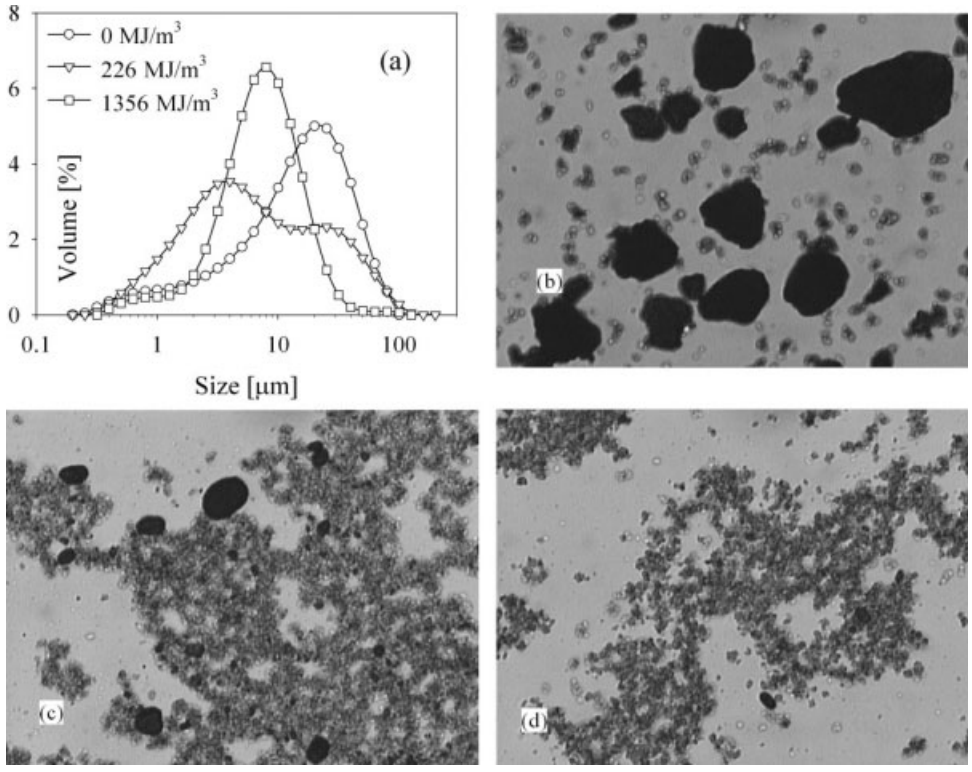

Figure 9. Transient size distributions (a) and morphology of hematite suspensions at (b) 0 MJ m^{-3}, (c) 226 MJ m^{-3}, and (d) 1356 MJ m^{-3}.

5 *w/w*% solid, 20 w/w_{solid}% Na-PAA and pH = 3; height of images 142 μm.

smaller, less compact aggregates (grey flocks on the images) were formed. At 1356 MJ m^{-3} all large, compact agglomerates disappeared and only smaller aggregates with the median diameter of the order of 10 μm were detected in the suspension. These results indicate that at pH = 3, the initial nanopowder can be dispersed into single nanoparticles/nanoaggregates however those nanoparticles are unstable and tend to reaggregate. Similar phenomena were observed at pH between 5 and 12 in aqueous suspensions of goethite nanoparticles.[6] Reaggregation of primary particles into relatively large, loosely packed aggregates can be explained by the reduction of electrostatic repulsive forces as indicated by the reduction of absolute value of zeta potential from 35 mV at pH = 4 to ~25 mV at pH = 3 and relatively high concentration of nanoparticles in suspension.

The effect of pH on zeta potential and on deagglomerate rate can be explained by different degree of dissociation of carboxylic acid groups and adsorption mechanisms of dispersant on particles surface at different pH. At pH = 3, those groups are very weakly ionized and absorbed on the surface by hydrogen bonding,[9,24] which leads to the reduction of zeta potential of hematite nanoparticles from 10 mV in water to −25 mV in the polymer solution. As pH increases to 4, the polymer ionization also increases and the dispersant is adsorbed on the surface by both chemical chelation and hydrogen bonding[25] and zeta potential of the suspension is reduced from −25 mV at pH = 3 to −35 mV at pH = 4. At this zeta potential deagglomeration rate was rather low (Figure 8). At pH above 8, the complete ionization is reached and the adsorption by chemical chelation[11] becomes predominant leading to further reduction of zeta potential from −35 mV at pH = 4 to −60 mV at pH = 9, for example to drastic increase of electrostatic repulsive forces which in turn leads to faster deagglomeration. Further increase of pH to 12 has no effect on zeta potential and on deagglomeration rate because full ionization of the polymer has already been reached.

Ravishankar et al.[26] and Nsib et al.[1] postulated weak adsorption of the polymer on the surface of hematite with a large number of long loops and tails providing an efficient steric repulsive interaction between hematite nanoparticles in the suspension at pH 8. At pH = 4, however, strong adsorption prevails with loops and tails closely attached to the surface giving thinner layer of adsorbed polymer and reducing steric repulsion. Although there is no direct evidence allowing quantification of the strength of binding between nanoparticles and polymer, the concept of charge stabilization is consistent with the polymer ionization theory and is supported by the measurements of zeta potential.

Rheological properties of hematite suspensions

Effect of Solid Concentrations. The flow curves at different concentrations of solid, measured immediately after the samples were taken are shown in Figure 10a.

Up to 20 *w/w%* solid the suspensions were Newtonian but at 30 *w/w%* solid the suspension became weakly shear thinning with power law index of 0.85 and with average apparent viscosity of 0.014 Pa s. The effect of solid concentration on viscosity of suspensions was correlated using MPQK equation[27,28]:

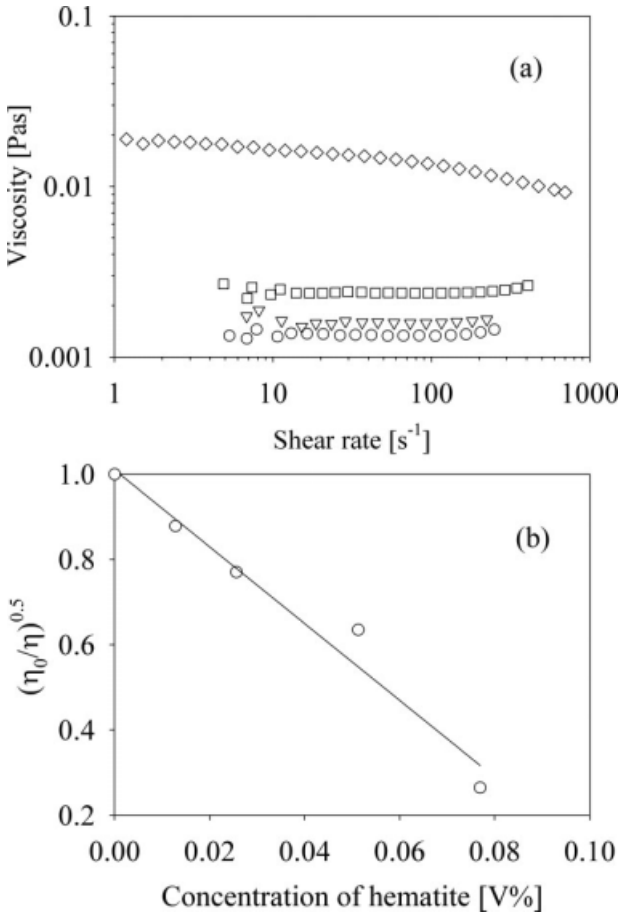

Figure 10. Rheology of hematite suspensions in 20 *w/w*$_{solid}$% Na-PAA solution at pH = 9 at different solid concentrations; (a) Flow curves, (○) 5 *w/w%*, (▽) 10 *w/w%*, (□) 20 *w/w%*, and (◇) 30 *w/w%* and (b) viscosity as function of volume fraction of solid, points—experimental data, line—best fit to Eq. 5.

$$\sqrt{\frac{\eta_0}{\eta}} = 1 - \frac{\phi}{\phi_m} \tag{5}$$

and the maximum volume packing fraction ϕ_m calculated from experimental data shown in Figure 10b by nonlinear regression was equal to 0.11 (weight fraction 0.4). Here, the viscosity of continuous phase (20 *w/w%* Na-PAA water solution) is around 1.25 mPa s. The results in Figure 10b indicate that MPQK model fits the experimental data rather well.

Effect of pH on Rheology of Suspension. Before the measurements of the rheology of suspensions, the rheology of 1% Na-PAA solution at different pH was measured. It has been found that at all pH (between 3 and 10), the solution was Newtonian with viscosity practically the same as viscosity of water. Therefore all the pH induced changes discussed later are caused by the changes of interparticle forces induced by changes of pH.

Effect of pH on rheological properties of the suspension of hematite nanoparticles is summarized in Figure 11.

At pH > 4, 5 *w/w%* suspensions were Newtonian with viscosity marginally higher than the viscosity of Na-PAA

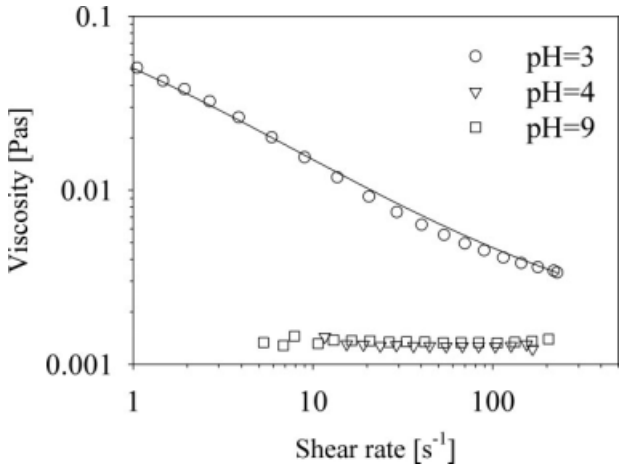

Figure 11. Rheology of 5 *w/w*% hematite nanopowder suspended in 20 w/w_{solid}% Na-PAA solution at different pH.

solution. However at pH = 3, viscosity of the suspension increased and the suspension became shear thinning. The effect of pH on rheology of the suspension of hematite nanoparticles is qualitatively similar to the effect of pH on rheology of the suspension of goethite nanoparticles.[6] Quantitatively, however, pH had much weaker effect on rheology of the suspension of hematite nanoparticles than on the rheology of the suspension of goethite nanoparticles. After the reduction of pH from 9 to 3, Newtonian suspension of hematite nanoparticles become weakly non-Newtonian ($n = 0.85$, $k = 0.242$ Pa s). The viscosity at the shear rate of 1 s^{-1} increased by less than two orders of magnitude. After the change of pH (from 3 to 9), the Newtonian suspension of goethite nanoparticles become very strongly shear thinning ($n \sim 0$ and $k = 6.9$ Pa s) and the viscosity at shear rate of 1 s^{-1} increased by five orders of magnitude. Such a drastic change of rheology has been discussed in details by the authors,[6] who postulated loosely packed porous agglomerates formed at pH = 3 (suspensions of hematite nanoparticles) or at pH > 3 (suspensions of goethite nanoparticles) trapped the water which led to an increase of "effective volume fraction of dispersed phase." Much stronger effect of pH on rheology of goethite suspensions can be explained by the fact that in those suspensions pH is the major factor controlling interparticle forces, whereas in hematite suspensions the Na-PAA determines the interparticle forces and reducing the effect of pH on those forces.

Reversibility of pH effect on rheology and morphology

To gain better understanding of the effect of pH on rheology and morphology of hematite suspensions the reversibility of the pH effect discussed earlier has also been investigated. The experimental procedure was described in details elsewhere[6] and it involved continuous monitoring of the pressure drop during the laminar flow of suspension through the pipe connecting stirred vessel and ultrasound cell while changing the pH. pH was changed stepwise first from 9 to 12, then from 12 to 3, and finally from 3 to 9 again as shown in Figure 12. At each pH very small samples were withdrawn and the particles size and morphology were analyzed. The results are shown in Figure 12.

The increase of pH from 9 to 12 followed by reduction from 12 to 5 did not affect pressure drop/viscosity. The suspension was water-like and the viscosity calculated from measured pressure drop and flow rate:

$$\eta = \frac{\pi \Delta P R^4}{8QL}. \tag{6}$$

was in rather good agreement with viscosity measured using rheometer (1.7 and 1.26 mPa s, respectively). The morphology was also practically unaffected with homogenously dispersed primary particles/small aggregates of 110 nm (Figure 12). When pH was reduced to 3 pressure drop increased within 2 min and irregular, loosely packed flocks were observed in a quiescent sample on a microscope slide. As pH was increased from 3 to 9 pressure drop decreased to the initial value and the

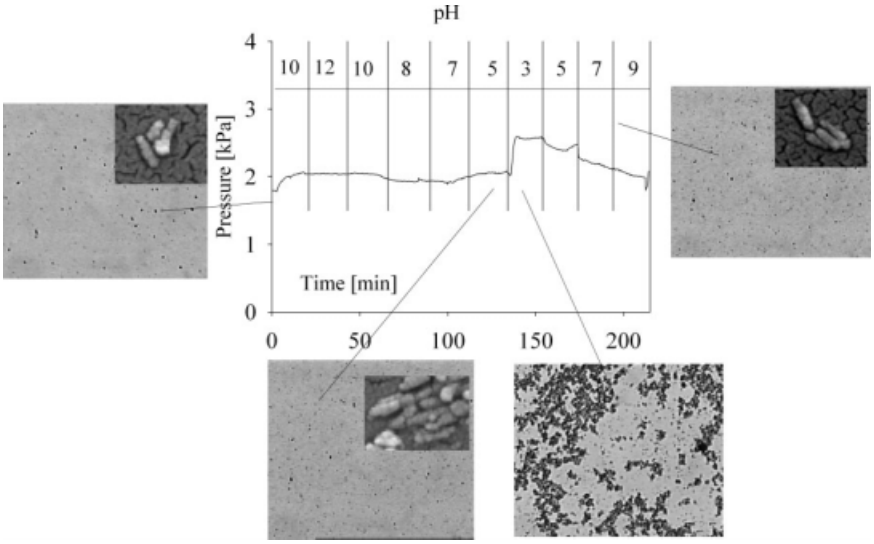

Figure 12. Reversibility of the effect of pH on morphology and rheology of the suspension of 5 *w/w*% hematite in 20 w/w_{solid}% NA-PAA solution.

Height of the image and the inset: 142 μm and 240 nm, respectively.

irregular, loosely packed flocks were redispersed into separate nanoparticles. However, this drop was far less sharp than the initial increase which indicates that the formation of flocks induced by changes of pH was much faster than breakage of those flocks. Again, qualitatively, very similar results were obtained for the suspension of goethite nanoparticles, but in this case, the increase of pressure/viscosity was five fold whereas in case of the suspension of hematite nanoparticles viscosity increased by <100%.

The results clearly show that the effect of pH on morphology and viscosity of hematite suspensions is reversible. This implies that the pH effect on ionization of Na-PAA and adsorption of Na-PAA on solid particles are also reversible, which could be exploited in processes involving formulation of different nanocomposite materials. The industrial exploitation of the effect of pH on rheology of the latex-nanoparticles during manufacturing of printer toners has been recently reported by the authors.[14,19]

Conclusions

The kinetics of deagglomeration of hematite nanopowder was similar to the kinetics of deagglomeration of goethite nanopowders with powders fracture and erosion as the main mechanisms of deagglomeration. Transient size distributions of aggregates were bimodal, therefore the kinetics of deagglomeration was described by cumulative volume fraction of nanoparticles (first mode of size distributions) and by reduction of median diameter of large aggregates caused by fracture (second mode of size distributions).

Fracture of large hematite aggregates required much higher energy input (critical energy density of the order of 100 MJ m^{-3}) than fracture of large goethite aggregates (critical energy density of the order of 10 MJ m^{-3}). At the same energy density, the volume fraction of eroded hematite nanoparticles was much lower than volume fraction of eroded goethite nanoparticles. Dispersion of the same mass of hematite nanopowder required nearly four times more energy than dispersion of goethite nanopowder.

Wet deagglomeration of hematite nanopowder into a stable suspension of single nanoparticles was only possible in the presence of dispersant. Deagglomeration of goethite nanopowder into stable suspension of nanoparticles only required pH of the order 3. Addition of Na-PAA to hematite suspensions at pH > 4 increased the absolute values of zeta potential and stabilized the suspensions by increasing repulsive electrostatic forces.

As the concentration of dispersant was increased from 1 to 5 w/w_{solid}%, the cumulative volume fraction of nanoparticles also increased but further increase to 10 and 20 w/w_{solid}% had no effect on cumulative volume fraction of nanoparticles. This implies that concentration necessary for full coverage is of the order of 5 w/w_{solid}% but much higher dispersant loads are common in industry.

The increase of solid concentration up to 20 to 30 w/w% reduced the amount of energy per unit mass of nanopowder necessary for complete dispersion of nanopowders. This can be explained by more efficient utilization of the energy of collapsing bubbles.[17]

The suspension of hematite nanoparticles in dispersant solution at pH = 3 was unstable and nanoparticles tend to reaggregate leading to an increase of viscosity of suspension. Similar behavior of the suspensions of goethite nanoparticles in water at pH between 5 and 12 was observed.

The effect of pH on rheology of the suspension of hematite nanoparticles is qualitatively similar to the effect of pH on rheology of the suspension of goethite nanoparticles.[6] Quantitatively, however, pH had much weaker effect on rheology of the suspension of hematite nanoparticles than on the rheology of the suspension of goethite nanoparticles. This can be explained by the fact that in goethite suspensions pH is the major factor controlling interparticle forces whereas in hematite suspensions the Na-PAA determines the interparticle forces and reduces the effect of pH on those forces. The pH effect on morphology and rheology of hematite and goethite suspensions is fully reversible.

Efficiency of deagglomeration was strongly dependent of pH and drastically increased as pH was increased from 4 to 9. Further increase of pH to 12 had practically no effect on fines generation.

Acknowledgements

This work is a part of PROFORM ("*Transforming Nanoparticles into Sustainable Consumer Products Through Advanced Product and Process Formulation*" EC Reference NMP4-CT-2004-505645) project, which is partially funded by the 6th Framework Program of EC. The authors acknowledge the useful discussions held with other partners of the Consortium: Bayer Technology Services GmbH; BHR Group Limited; Centre for Computational Continuum Mechanics (C3M); Karlsruhe University, Inst. of Food Process Eng; Loughborough University, Department of Chemical Eng; Poznan University of Technology, Inst. of Chemical Technology and Eng; Rockfield Software Limited; Unilever UK Port Sunlight, Warsaw University of Technology, Department of Chemical and Process Eng.

Notation

C = constant, μm $MJ^{-\alpha}$ $m^{3\alpha}$
d_{50} = median diameter of aggregates, m
E_V = energy input per volume of suspension, MJ m^{-3}
E_W = energy input per mass of solid, MJ kg^{-1}
f_p = cumulative volume fraction of fine particles
L = length between two pressure indicators, m
P = power input, W
ΔP = pressure drop in pipe, kPa
R = radius of pipe, m
t_r = mean residence time in flow cell, s
t_t = processing time, s
V_{cell} = volume of flow cell, m^3
V_t = volume of suspension, m^3
W_s = mass of solid, kg
α = constant
β = constant
ϕ = volume fraction of solid
ϕ_m = volume fraction of maximum packing solid
η = viscosity of suspension, Pa s
η_0 = viscosity of Newtonian continuous phase, Pa s

Literature Cited

1. Nsib F, Ayed N, Chevalier Y. Dispersion of hematite suspensions with sodium polymethacrylate dispersants in alkaline medium. *Colloids Surf A Physicochem Eng Asp.* 2006;286:17–26.
2. Stoffer JO, Fahim M. Ultrasonic dispersion of pigment in water based paints. *J Coat Technol.* 1991;63:61–68.
3. Jorge E, Chartier T, Boch P. Ultrasonic dispersion of ceramic powders. *J Am Ceram Soc.* 1990;73:2552–2554.
4. Iler RK. *The Chemistry of Silica: Solubility, Polymerization, Colloid and Surface properties, and Biochemistry*. New York: Wiley, 1979.

5. Pacek AW, Ding P, Utomo AT. Effect of energy density, pH and temperature on de-aggregation in nano-particles/water suspensions in high shear mixer. *Powder Technol*. 2007;173:203–210.
6. Ding P, Pacek AW. Effect of pH on deagglomeration and rheology/morphology of aqueous suspensions of goethite nanopowder. *J Colloid Interface Sci*. 2008;325:165–172.
7. Reuter E, Silber S, Psiorz C. The use of new blockcopolymeric dispersing agents for waterborne paints—theoretical and practical aspects. *Progress Org Coat*. 1999;37:161–167.
8. Vermohlen K, Lewandowski H, Narres HD, Koglin E. Adsorption of polyacrylic acid on aluminium oxide: DRIFT spectroscopy and ab initio calculations. *Colloids Surf A Physicochem Eng Asp*. 2000;170:181–189.
9. Foissy A, Attar AE, Lamarche JM. Adsorption of Polyacrylic-Acid on Titanium-Dioxide. *J Colloid Interface Sci*. 1983;96:275–287.
10. Banash MA, Croll SG. A uantitative study of polymeric dispersant adsorption onto oxide-coated titania pigments. *Prog Org Coat*. 1999;35:37–44.
11. Zaman AA, Tsuchiya R, Moudgil BM. Adsorption of a low-molecular-weight polyacrylic acid on silica, alumina, and kaolin. *J Colloid Interface Sci*. 2002;256:73–78.
12. Stenkamp VS, Berg JC. The role of long tails in steric stabilization and hydrodynamic layer thickness. *Langmuir*. 1997;13:3827–3832.
13. Washburn EW. *International Critical Tables of Numerical Data, Physics, Chemistry and Technology*, 1st electronic ed. New York: Knovel, 2003.
14. Ding P, Pacek AW, Abinhava K, Pickard S, Edwards MR, Nienow AW. A process for the manufacture of chemically produced toner (CPT). II. Effect of operating conditions. *Ind Eng Chem Res*. 2005;44:6012–6021.
15. Holmberg K. *Handbook of Applied Surface and Colloid Chemical*. West Sussex: Wiley, 2002. p. 1–2.
16. Cornell RM, Schwertmann U. *The Iron Oxides, Structure, Properties, Reactions, Occurrence and Uses*. Wiley-VCH: Weinheim, 1996.
17. Ding P, Pacek AW. De-agglomeration of goethite nano-particles using ultrasonic comminution device. *Powder Technol*. 2008;187:1–10.
18. Kusters KA, Pratsinis SE, Thoma SG, Smith DM. Energy-size reduction laws for ultrasonic fragmentation. *Powder Technol*. 1994;80:253–263.
19. Ding P, Pacek AW, Abinhava K, Pickard S, Edwards MR, Nienow AW. A process for the manufacture of chemically produced toner (CPT). I. Evolution of structure and rheology. *Ind Eng Chem Res*. 2005;44:6004–6011.
20. Gao MW, Forssberg E. Prediction of product size distributions for a stirred ball mill. *Powder Technol*. 1995;84:101–106.
21. Mende S, Stenger F, Peukert W, Schwedes J. Mechanical production and stabilization of submicron particles in stirred media mills. *Powder Technol*. 2003;132:64–73.
22. Kusters KA, Pratsinis SE, Thoma SG, Smith DM. Ultrasonic fragmentation of agglomerate powders. *Chem Eng Sci*. 1993;48:4119–4127.
23. Mosquet M, Chevalier Y, Le Perchec P, Foissy A, Guicquero JP. The mechanism of fluidization of concentrated calcium carbonate slurries by poly(oxyethylene) diphosphonates. *Colloid Polym Sci*. 1999;277:1162–1171.
24. Cesarano J, Aksay IA, Bleier A. Stability of aqueous alpha-Al2O3 suspensions with poly(methacrylic acid) poly-electrolyte. *J Am Ceram Soc*. 1988;71:250–255.
25. Gebhardt JE, Fuerstenau DW. Adsorption of polyacrylic-acid at oxide water interfaces. *Colloids Surf*. 1983;7:221–231.
26. Ravishankar SA, Pradip, Khosla NK. Selective flocculation of iron-oxide from its synthetic mixtures with clays—a comparison of polyacrylic-acid and starch polymers. *Int J Mineral Process*. 1995;43:235–247.
27. Quemada D. Rheology of concentrated disperse systems and minimum energy-dissipation principle. I. Viscosity-concentration relationship. *Rheol Acta*. 1977;16:82–94.
28. Kitano T, Kataoka T, Shirota T. An empirical-equation of the relative viscosity of polymer melts filled with various inorganic fillers. *Rheolog Acta*. 1981;20:207–209.
29. Alexander S. Adsorption of chain molecules with a polar head a-scaling description. *J Phys*. 1977;38:983–987.
30. Degennes PG. Conformations of polymers attached to an interface. *Macromolecules*. 1980;13:1069–1075.
31. Degennes PG. Polymers at an interface—a simplified view. *Adv Colloid Interface Sci*. 1987;27:189–209.

Manuscript received Nov. 26, 2008, and revision received Feb. 10, 2009.